Journal of Physics: Conference Series **1643** (2020) 012085 doi:10.1088/1742-6596/1643/1/012085

# Inclusive breakup measurements of the $^{7}$Li+ $^{119}$Sn reaction.

**J. P. Fernández-García [1,2], M. A. G. Alvarez[1], S. Cherubini[3,4], A. Di Pietro[3], G. D'Agata[3,4], B. Fernández[2], P. Figuera[3], M. Fisichella[3], M. Giulino[3,5], M. La Cognata[3], L. Lamia[3,4], M. Lattuada[3,4], J. Lei[6], A. M. Moro[1], R. G. Pizzone[3], D. Santonicito[3], R. Sparta[3], A. Tumino[3,5], A. C. Shotter[7] and M. Zadro[8]**

[1]Departamento de FAMN, Universidad de Sevilla, Apartado 1065, E-41080 Seville, Spain. [2]Centro Nacional de Aceleradores, Universidad de Sevilla, Junta de Andalucía-CSIC, 41092 Sevilla, Spain. [3]INFN, Laboratori Nazionali del Sud, via S. Sofia 62, 1-95123 Catania, Italy. [4]Dipartamento di Fisica e Astronomia, via S. Sofia 64, I-95123 Catania, Italy. [5]Facoltà di Ingegneria ed Architettura, Università Kore, I-94100 Enna, Italy. [6]Institute of Nuclear and Particle Physics, and Department of Physics and Astronomy, Ohio University, Athens, Ohio 45701, USA. [7]School of Physics and Astronomy, University of Edinburgh, Edinburgh, UK. [8]Ruder Bošković Institute, Zagreb, Croatia.

E-mail: jpfernandez@us.es

**Abstract.** We present preliminary data of elastic scattering and inclusive breakup cross sections for the $^{7}$Li+ $^{119}$Sn reaction, recently measured at the Laboratori Nazionali del Sud (LNS-INFN) (Catania, Italy) at energies around the Coulomb barrier ($E_{lab}$ = 21.2 and 26.5 MeV). The experimental data have been analyzed under the Optical Model and Continuum-Discretized Coupled-Channels methods.

## 1. Introduction.

The study of collisions induced by halo nuclei has revealed that its diffuse structure associated with a very low breakup threshold has an effect in the reaction dynamic (see e.g. [1] and references therein). Due to the low binding energy, the dissociation of the projectile into two or more fragments is an important mechanism occurring in collisions induced by these radioactive nuclei and coupling effects to the continuum deeply affect the other reaction channels around the barrier. The stable weakly bound nucleus, $^{7}$Li, has similar characteristics as halo nuclei, such as a low breakup threshold ($S_{\alpha}$=2.47 MeV) associated with a marked cluster structure of the ground state ($\alpha + t$). Therefore, the coupling to the breakup channels can affect the dynamics of reactions induced by these nuclei (see, e.g., Refs. [1, 2, 3]). The study of reactions induced by stable weakly bound nuclei (where good quality data are easier to obtain due to the higher beam intensity) enables to extract structural information of the projectile and to check the validity of new models which will also help in understanding the reaction dynamics with halo nuclei.

We present preliminary results of the elastic scattering for the $^{7}$Li+ $^{119}$Sn reaction as well as the $\alpha$ and $t$ cross sections produced in the breakup of the projectile. The experimental data have been compared with a global optical model potential and with the Continuum-Discretized Coupled-Channels (CDCC) calculations.

## 2. Experimental set-up.

The measurements of the elastic scattering angular distributions for $^{7}$Li on $^{119}$Sn were performed at the Laboratori Nazionali del Sud as a complementary study of Ref. [4], where the fusion excitation function of the same system was obtained for a wide energy range around the Coulomb barrier. The $^{7}$Li beam was produced by the SMP Tandem Van de Graaff accelerator and transported to the CT2000 scattering chamber.

Charged particles coming from the reactions were detected and identified by five triple-silicon telescopes. Each telescope was composed by a ∼15 $\mu$m thick detector ( $\Delta$E1) plus a ∼150 $\mu$m thick detector ( $\Delta$E2) and a detector with a thickness of ∼1000 $\mu$m(E). The telescope systems were mounted on a rotating plate. The angular distributions were measured at steps of 10° in the angular ranges $\theta_{lab}$=40° - 160° using three angular settings. In the first angular setting the detectors covered an angular range between 40° - 80° and the target was placed at 65° with respect to the beam direction, while in the second and third angular setting the target was positioned at 125° and the angular range was 80° - 120° and 120° - 160°, respectively (see Table 1). The $^{119}$Sn target thickness was around 280 $\mu$g/cm$^2$.

**Table 1.** Angular position of each telescope in set I, II and III.

| Telescope | Set I | Set II | Set III |
|---|---|---|---|
| 1 | 40° | 80° | 120° |
| 2 | 50° | 90° | 130° |
| 3 | 60° | 100° | 140° |
| 4 | 70° | 110° | 150° |
| 5 | 80° | 120° | 160° |

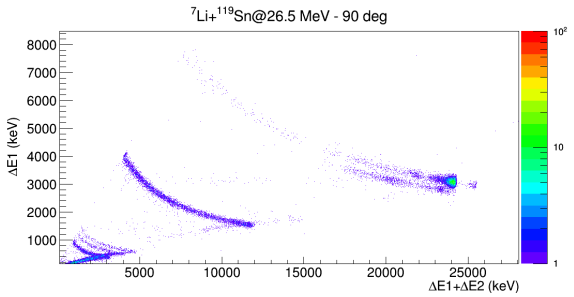


**Figure 1.** Bidimensional diagram $\Delta$E1 versus $\Delta$E1 +$\Delta$E2 of the reaction $^{7}$Li+$^{119}$Sn at 26.5 MeV.

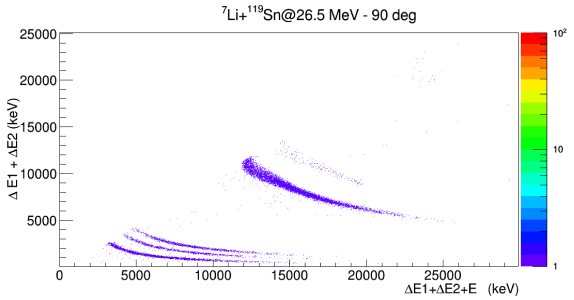


**Figure 2.** Bidimensional diagram $\Delta$E1 +$\Delta$E2 versus $\Delta$E1 +$\Delta$E2 + E of the reaction $^{7}$Li+$^{119}$Sn at 26.5 MeV.

Circular collimators with diameters of 6 mm were positioned in front of each telescope, in such a way that their angular opening with respect to the target center was ∼1.0°. Two monitor detectors with a 3 mm collimator, placed at ±20° were used for normalization purposes. The ratio of the solid angles of the monitors and telescopes was determined by the Rutherford scattering of $^{7}$Li on a ∼110 $\mu$g/cm$^2$ $^{197}$Au target. Two examples of bidimensional diagrams $\Delta$E1 versus $\Delta$E1 +$\Delta$E2 and $\Delta$E1+$\Delta$E2 versus $\Delta$E1+$\Delta$E2+E of the reaction $^{7}$Li+$^{119}$Sn at 26.5 MeV are represented in Figs. 1 and 2. A remarkable separation in mass and charge of the different reaction products is observed.

The ratio of the elastic scattering to the Rutherford cross section is obtained from the following expression [5],

$$\frac{d\sigma_{El}}{d\sigma_{Ruth}}(\theta) = \frac{N_{det}(\theta_{det})}{N_{mon}(\theta_{mon})} \cdot \frac{(d\sigma_{Ruth}/d\Omega)(\theta_{mon})}{(d\sigma_{Ruth}/d\Omega)(\theta_{det})} \cdot \frac{N^{Au}_{mon}(\theta_{mon})}{N^{Au}_{det}(\theta_{det})} \cdot \frac{(d\sigma_{Ruth}/d\Omega)^{Au}(\theta_{det})}{(d\sigma_{Ruth}/d\Omega)^{Au}(\theta_{mon})}, \quad (1)$$

where,

$$\frac{N^{Au}_{mon}(\theta_{mon})}{N^{Au}_{det}(\theta_{det})} \cdot \frac{(d\sigma_{Ruth}/d\Omega)^{Au}(\theta_{det})}{(d\sigma_{Ruth}/d\Omega)^{Au}(\theta_{mon})} = \frac{\Delta\Omega_{mon}}{\Delta\Omega_{det}}. \quad (2)$$

$N_{mon}(\theta_{mon})$ and $N_{det}(\theta_{det})$ are the number of events detected in the monitor detector and in the telescope at angle $\theta_{det}$, respectively, and $\Delta\Omega_{mon}$and $\Delta\Omega_{det}$ are the corresponding solid angles.

In Fig. 3, preliminary experimental data of the elastic cross section angular distributions are presented. Moreover, in Figs. 4 and 5, the angular distributions of the $\alpha$ and $t$ particles coming from the breakup of the $^7$Li projectile are showed.

## 3. Theoretical calculations and preliminary results.

Elastic scattering angular distributions are compared with optical model calculations using the global potential $^7$Li-target of Ref. [6]. The parameters of this potential are given in Tab. 2. A good agreement between the OM calculations, represented by solid black lines, and the experimental data is observed in Fig. 3.

On the other hand, elastic scattering and breakup angular distributions for $^7$Li on $^{119}$Sn target have been simultaneously analyzed within CDCC formalism. This method has been successfully applied to describe reactions induced by halo and weakly bound nuclei, such as $^{6,7,11}$Li, $^{11}$Be and $^6$He [3, 7, 8, 9, 10, 11, 12, 13, 14]. We would like to emphasize that this calculation only considers the elastic breakup of the projectile, where the projectile fragments, $\alpha$ and $t$, and the target remain in their ground state. All other breakup mechanisms, called non-elastic breakup, such as inelastic excitation of target or fragments, particle transfer and incomplete fusion, are not included.

As in Ref. [3], the $^7$Li isotope was described as an $\alpha$+$t$ system, with a breakup threshold at 2.47 MeV. The excited state $1/2^-$, the resonances $7/2^-$ and $5/2^-$ and the non-resonant states were considered. The calculated elastic scattering, $\alpha$ and $t$ breakup angular distribution are represented by the red dashed line in Figs. 3, 4 and 5, respectively. Unlike the calculated elastic scattering, where the CDCC calculations reproduce the experimental data, the $\alpha$ particles angular distributions coming from the breakup of the projectile as well as the $t$ particles cannot be described by a elastic breakup mechanism, suggesting that other breakup mechanisms need to be considered.

**Table 2.** Parameters of the optical potential $^7$Li+$^{119}$Sn. The Coulomb radius is $R_C$=6.394 fm

| $V_v$ | $R_v$ | $a_v$ | $W_i$ | $R_i$ | $a_i$ |
|---|---|---|---|---|---|
| 114.2 | 6.325 | 0.853 | 12.72 | 8.554 | 0.809 |

## 4. Conclusions.

Preliminary experimental data of the elastic scattering angular distribution as well as the $\alpha$ and $t$ particles coming from the breakup of the $^7$Li projectile have been presented at two energies

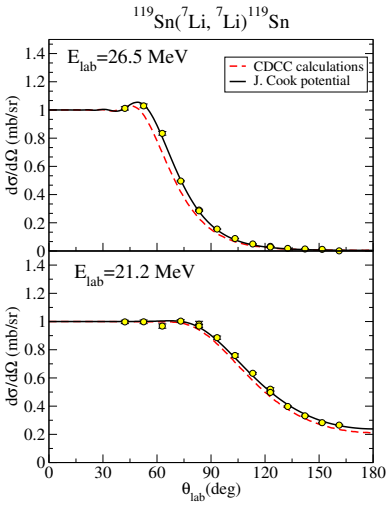


**Figure 3.** Elastic scattering angular distributions.

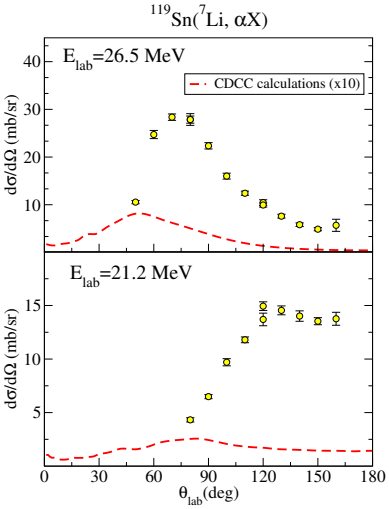


**Figure 4.** $\alpha$ cross section angular distributions.

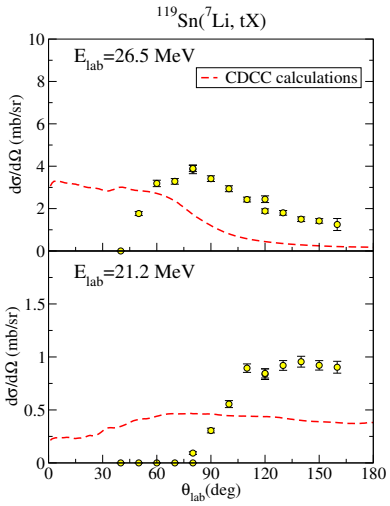


**Figure 5.** $t$ cross section angular distributions.

21.2 and 26.5 MeV around the Coulomb barrier. The elastic scattering angular distributions have been analyzed under the optical model framework, where the global potential of Ref. [6] reproduces the experimental data.

The elastic scattering and the $\alpha$ and $t$ cross sections have been simultaneously studied with the CDCC formalism. Although the elastic scattering cross sections are well reproduced by the CDCC calculations, the calculated $\alpha$ and $t$ cross sections are found to largely underestimate the experimental data, indicating that the observed breakup fragments are not produced by an elastic breakup mechanism.

New calculations based on a re-examination of the inclusive breakup cross-section model proposed by Ichimura, Austern and Vincent [15], where a formal separation between the elastic breakup and non-elastic breakup contributions is considered [16], are in progress.

**Acknowledgements**

This work was partially supported by the Spanish Ministerio de Ciencia, Innovación y Universidades and FEDER funds (Project No. PGC2018-096994-B-C21) and by the European Unions Horizon 2020 research and innovation program under Grant Agreement No. 654002.

**References.**

[1] Canto L F, Gomes P R S, Donangelo R and Hussein M S 2006 *Phys. Rep.* **424** 1
[2] Thompson I J and Nagarajan M A *Phys. Lett. B* **106** 163 – 166
[3] Fernández-García J P *et al.* 2015 *Phys. Rev. C* **92**(5) 054602
[4] Fisichella M *et al.* 2017 *Phys. Rev. C* **95**(3) 034617
[5] Zadro M *et al.* 2009 *Phys. Rev. C* **80** 064610
[6] Cook J *et al.* 1982 *Nucl. Phys. A* **388** 173
[7] Di Pietro A *et al.* 2010 *Phys. Rev. Lett.* **105** 022701
[8] Cubero M *et al.* 2012 *Phys. Rev. Lett.* **109** 262701
[9] Di Pietro A *et al.* 2004 *Phys. Rev. C* **69** 044613
[10] Acosta L *et al.* 2011 *Phys. Rev. C* **84** 044604
[11] Fernández-García J P *et al.* 2013 *Phys. Rev. Lett.* **110** 142701
[12] Fernández-García J P *et al.* 2015 *Phys. Rev. C* **92**(4) 044608
[13] Sakuragi Y 1987 *Phys. Rev.* **C35** 2161
[14] Fernández-García J P *et al.* 2019 *Phys. Rev. C* **99**(5) 054605
[15] Ichimura M, Austern N and Vincent C M 1985 *Phys. Rev. C* **32** 431

[16] Lei J and Moro A M 2015 *Phys. Rev. C* **92** 044616